Stony Brook University

The Effect of Nanoparticles on the Properties of Polystyrene Dead Layers

A Thesis Presented

by

Yuxuan Ruan

to

The Graduate school

in Partial Fulfillment of the

Requirements

for the Degree of

Master of Science

in

Materials Science and Engineering

Stony Brook University

May 2012

Stony Brook University

The Graduate school

Yuxuan Ruan

We, the thesis committee for the above candidate for the

Master of science degree, hereby recommend

acceptance of this thesis.

Tadanori Koga – Thesis Advisor
Assistant Professor, Materials Science and Engineering

Michael Dudley – Committee Member
Professor, Materials Science and Engineering

T. A. Venkatesh– Committee Member
Assistant Professor, Materials Science and Engineering

This thesis is accepted by the Graduate school

Charles Taber
Interim Dean of the Graduate school

Abstract of the Thesis

The Effect of Nanoparticles on the Properties of Polystyrene Dead Layers

by

Yuxuan Ruan

Master of Science

in

Materials Science and Engineering

Stony Brook University

2012

A polymer dead layer is a very thin interfacial layer of polymer formed at the solid substrate interface, with no thermal expansion coefficient and molecular mobility. The polymer dead layer has many unique properties compared to the bulk polymer, including the mobility of polymer chains, glass transition temperature, viscosity and so on. In this thesis, organic clay nanoparticles are used as a nanofiller to see how the properties/structures a polystyrene dead layer can be altered. To characterize the structures of PS/clay dead layers, we used ellipsometry, X-ray scattering techniques, and atomic force microscopy (AFM). In addition, supercritical carbon dioxide was used as a screening solvent to control the polymer/substrate interactions.

Table of Contents

List of Figures

The Effect of Nanoparticles on the Properties of Polystyrene Dead Layers

Chapter 1 Introduction

1.1 Effect of nanoparticles on polymer nanocomposites

For better life experience, people nowadays are looking for new materials that have better properties than traditional materials, and polymers are one of those novel materials. However, sometimes even different kinds of pure polymers cannot meet the demand of applications. People begins to add nanoparticles to polymers to get nanocomposites. A nanocomposite is a composed material in which has one or more dimensions at least one component has a nano-scale size. With a small amount of nanofillers added to the polymer matrix, some properties of the polymer nanocomposite systems were found to change significantly, for example, mechanical properties, electrical properties, gas permeability, flame retardant etc. This means the understanding of the interactions between nanoparticles and polymers is the key to control these properties. Polymer nanocomposites have attracted tremendous attention in both academic and industry areas. Kashiwagi et al. [1] mentioned that polyamide-clay nanocomposites have good thermal stability and better flame retardant than pure polyamide, and they believe that a particles with a large aspect ratio such as clay has an advantage because it forms better network-like structures in a polymer than particles with a small aspect ratio. Ahn et al. [2] studied the gas separation behavior of polysulfone by characterizing the thermal properties of silica-filled polysulfone and the results show that the T_g of silica-filled polysulfone is slightly higher than that of pure polysulfone, which means that a confined polymer region formed due to the increase of stress at the polymer-silica interface. In addition, the gas permeability of silica-filled polysulfone was tested and the results indicated that the gas permeability of silica-filled polysulfone is higher than that of the unfilled polysulfone. The reason is the introduction of the nanoparticles increases the total free volume of the system by disrupting the packing of polymer chains. Kim et al. [3] studied on waterborne polyurethane/clay nanocomposite, proving that the mechanical properties, thermal and water resistance were enhanced by organic clay, and the unique mechanical property is more evident when the tests were performed at above T_g and with large deformation. These different properties mentioned above result from the properties of nanoparticles embedded in polymers, such as the dimension, microstructure and orientation [4] of nanoparticles. There are many different kinds of nanoparticles, for example, exfoliated graphite, carbon nanotubes, carbon nanofillers, nanocrystaline metals and nano fibers [5].

1.2 Clay nanoparticles

The inexpensiveness of clay nanoparticle makes it a very popular filler and people

can make nanocomposite materials at a low cost. In addition, compared to conventional nanofillers, clay has a very low fraction of filler addition [6]. Clay is a kind of regular stacks of aluminosilicate layers contains layered perovskites, graphite intercalation compounds, and it has a high aspect ratio and high surface area. The individual clay layers can have big improvements in different polymer properties due to high interfacial interactions with polymer. With sonication, clay can exfoliate into platelets, the minimum thickness is about 1 nm, but the lateral dimension of clay may vary from 30 nm to several microns depending on the source and the method of preparation the clay. The structure of a typical clay is shown in Fig. 1-1 [5, 7, 8]. The tetrahedral sheets are built from a silicon atom in the center which is surround by four oxygen atoms, while the octahedral sheets have aluminum or magnesium atoms in the center and surrounded by eight oxygen atoms. Actually the tetrahedral parts and the octahedral parts are sticking together by sharing these oxygen atoms. There are mainly two kinds of clay structures, one tetrahedral part fused with one octahedral part is known as 1:1 kaolin group, and the main composition is $Al_2Si_2O_5(OH)_5$. The other type of clay has one octahedral part fused with two tetrahedral parts, which is called a 2:1 layered silicate structure, also known as phyllosilicates. If there are no inter layer ions, the layers will not expand in water. If the silicon atom in the tetrahedral structure is replaced by aluminum atom, the 2:1 structure is known as mica. There will be a negative charge induced by this replacement, but the negative charge will be neutralized by the potassium cations between layers. The 2:1 layers hold very firmly so that the exfoliation of layers is difficult. If the aluminum cations are partially replaced by divalent magnesium, the layers are called a smectite clay group. This replacement also cause a negative charge, and is balanced by inter layer calcium ions. The size of inter layer cations is not always the same as holes of tetrahedral sheets, and the layers stay close and have a regular gap between them, which is called inter layer or gallery. The force holding the layers together are van der waals forces and electrostatic, which are relatively weak. Also the distance between layers varies due to different charge density on the layers, cation radius and degree of hydration. The cations between layers can be hydrated in solutions, which is called clay swelling. The swelling of clay leads to the increase of inter layer space. So polymer chains can intercalate in hydrated clay, which has inter layer spacing and weak inter layer forces, and the lattice of layers will expand and finally lead to the separation of each layer. The special exfoliation and intercalation behavior of clay makes it a high aspect ratio filler, which is very efficient and promising when preparing nanocomposites with polymeric materials [9].

The individual clay layer has 1-3 nm thickness and its structure has huge effects on the properties of polymers. The higher the surface in dispersed structure, the stronger the force between layers is. This means layers have more tendency to aggregate and the agglomeration of layers is easier. Multiple parallel layers together with thickness around

10nm are called “primary clay particles”. The aggregations of clay are formed by joining “primary clay particles” randomly.

The intrinsic water solubility of clay is high, while most of the polymers are hydrophobic. This will prevent the dispersion of clay within the polymer matrix and lead to a weak interaction between clay and the polymer. This incompatibility between hydrophilic clay and polymer will hinder the exfoliation of clay and preparation of well dispersed nanocomposites with better properties. Scientists have been modifying clay by adding hydrophobic agents to the surface of clay [5], making the surface energy of clay decrease. The modification of clay makes clay reduce surface energy of the clay and allows them to disperse in a polymer matrix easily. The interaction between polymer and clay is enhanced. Clay 6A, 20A, 25A, 30A are typical organically-modified clay. The difference between different types of clay is the concentration of ammonium salt, i.e., the concentration of ammonium salt in clay 6A is 140 meq /100 g and that for clay 20A is 95 meq /100 g. [6]

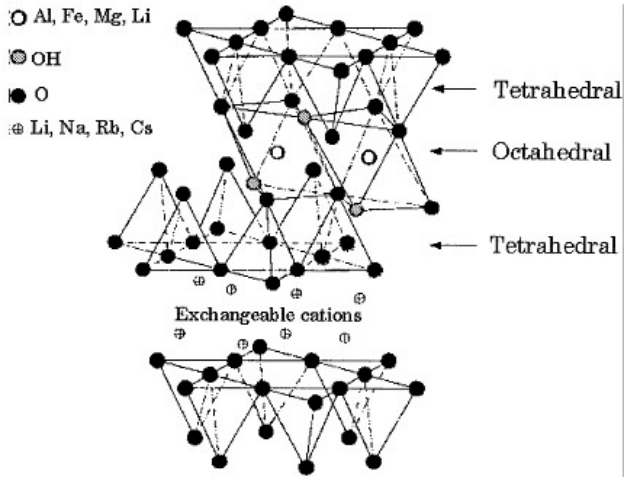

Figure 1-1. Scheme of 2 : 1 smectite clay structure [5]

1.3 Interaction between polymer and clay

It is crucial to achieve exfoliation of clay nanoparticles in order to prepare polymer-clay nanocomposite films. The common method to make homogenously dispersed polymer-clay nanocomposite is to mix a polymer and clay together, using a good solvent for the polymer and organo clay. When a polymer does not dissolve well at room temperature, the mixture will be heated above the softening point of the polymer [10]. During this process, polymer chains diffuse into the solvent and go into the galleries of clay platelets to form intercalated or exfoliated structure, as seen in Fig. 1-2 [11]. For the intercalated case, the polymer is inserted in the space between clay layers and the

inter-layer spacing is increased, but layers still have good spatial relationship with each other. As for the exfoliated case, however, clay layers are completely separated and randomly distributed throughout the whole system [12].

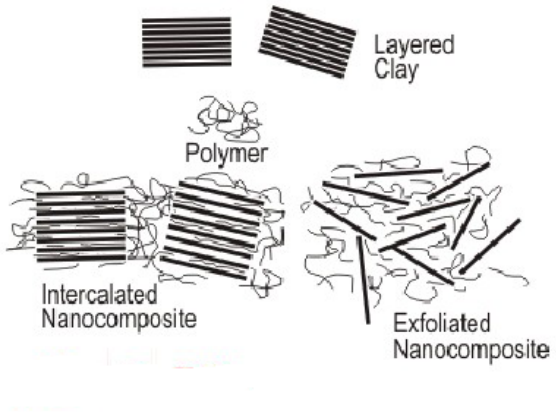

Figure 1-2. Formation of intercalated and exfoliated nanocomposites from layered silicates and polymers [11].

1.4 Polymer thin film and dead layer

With the growing interest of nanoscale devices, mechanical and thermodynamic properties of nano-materials are now of importance. Many results show that the properties and structures of nanoscale thin films can be hugely different from those of the bulks [13-16]. In the study of the glass transition temperature (T_g) of thin film by Keddie et al. [13], it was shown that the T_g of nanoscale thin film was lower than the bulk. Reiter et al. [14] also mentioned that the dewetting of polymer thin films was observed below bulk T_g, suggesting the effective T_g of thin films was lower than that of the bulk value. Tsui et al. [15] obtained research results on the elastic modulus of polystyrene (PS) spin cast thin film is obviously smaller than bulk. These deviations in thermodynamic and mechanical properties from the bulk are very important for the applications of polymer thin films. However, there are also opposite experimental results showing that the T_g of polymer thin film is higher than that of bulk. Wallace et al. [17] used X-ray reflectivity and showed that the T_g of PS thin film is higher than the bulk value. These two totally different results were further studied by using Auger electron spectroscopy by Wallace, and the reason is that Keddie used silicon with native-oxide surface as the substrate while Wallace used hydrofluoric acid to etch away the native-oxide layer. This is important to bring up the effect of the substrate surface on the behavior of polymer thin films.

A polymer dead layer (also called residual layer or absorbed layer [18-21]) is a very thin interfacial polymer layer at the substrate, and in most cases this thin layer has no thermal expansion coefficient or molecular mobility [22, 23]. The reason why dead layers are becoming interesting is that the interface of a hybrid material based on organic and

inorganic materials affects the final performance of this material. The most common method to prepare a polymer dead layer is using a good solvent to wash a polymer thin film, and the final remained polymer layer is the dead layer. Fujii et al. [18] spun cast PS thin films on silicon substrates and washed PS layers by toluene for 10 mins, until the residual thickness remained unchanged.

1.5 Literature review on dead layers

1.5.1 Annealing time dependence of dead layer thickness

The most critical issue about the polymer dead layer is how annealing time affects the growth of the polymer. Fujii et al. [18] have shown thickness dependence of PS dead layers as a function of the annealing time with M_w ranging from 13.7 K to 940 K. The PS samples were spun cast on clean silicon substrates and annealed at 150 ℃ in air with different annealing times. The original thickness of the PS thin film was 200nm. After annealing, the films were submerged in toluene to remove the top mobile layer, then a very thin layer of PS left on the silicon substrate is a dead layer. The thickness of each dead layer was determined by ellipsometry. The results show that as the increase of the annealing time, the thickness of the dead layers increases and will finally reach the equilibrium, as shown in Fig. 1-3.

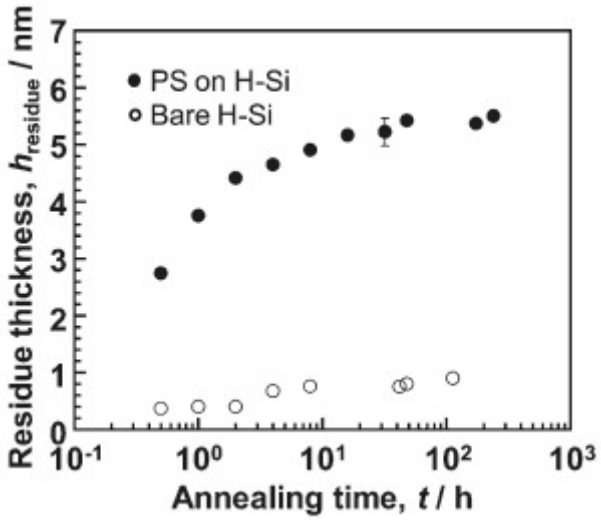

Figure 1-3. Annealing time dependence of the thickness of the dead layer, The annealing was carried out at 150 ℃ in air. The molecular weight of PS is M_w = 44.1 kg/mol. The solid circles are the thickness data of PS dead layer on the Si substrate and the open circles are the thickness of Si substrate (washed with HF) with no PS. The PS dead layer is more than six times thicker than that of the Si. The saturation of the PS dead layer happened at about 50 h annealing time while the Si thickness saturated around 4 h. [18]

Fujii et al. further focused on the effect of radius of gyration (R_g, mean-square distance of a chain segment from the center of mass of the molecule) on the thickness of the dead layers. The R_g dependence shows that the higher the R_g value is, the thicker the dead layer is. Moreover, the comparison between the dead layer on Si and on SiO_x/Si illustrates that even the affinity of PS to different substrates are different, the results show the same trend. The final thickness of the dead layer of PS/Si is about $0.81R_g$, and for PS/ SiO_x is 0.47 R_g. (Fig. 1-4)

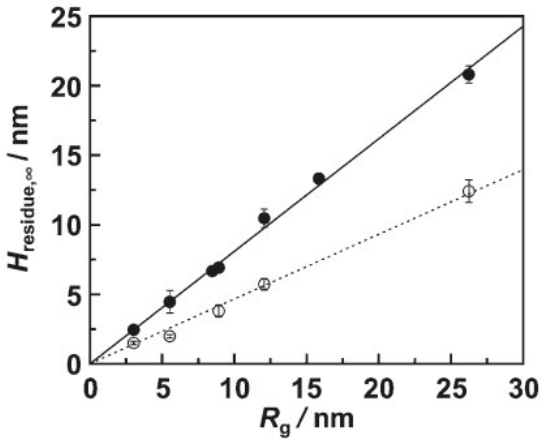

Figure 1-4. Dependence of dead layer thickness on R_g. Solid circles stand for the PS/Si system, open circles stand for PS/ SiO_x system. The thickness of PS/ SiO_x dead layer is 58% of the thickness of PS/Si. [18]

1.5.2 How annealing time affect the T_g of polymer dead layer

Another topic about the polymer dead layer is how T_g changes with increasing annealing time. Napolitano et al. [20] showed that the polymer dead layer has significant impact on the T_g of PS. They prepared PS films using spin-casting on aluminum substrates. The result shows that T_g of the dead layer is different from that of bulk PS. PS (M_w = 97K) dead layers prepared at different annealing time have different T_g, at short annealing time (around 3 h), T_g of the dead layer is about 5 K lower than the bulk T_g, and the T_g increases until it reaches an equilibrium temperature, which is about 7 K higher than bulk T_g. Similar behavior is also observed for ultrathin films. (Fig. 1-5)

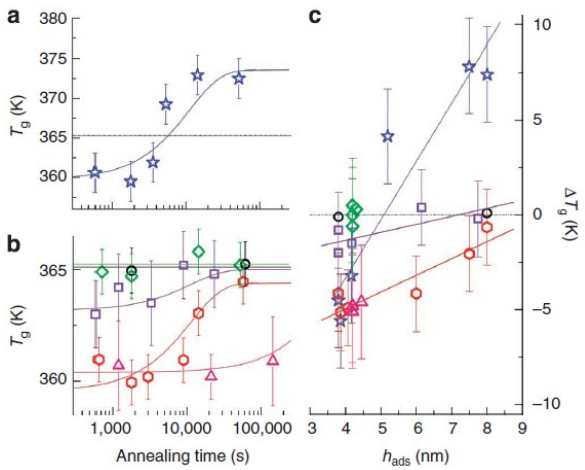

Figure 1-5. Time evolution of the T_g of films of PS (M_w = 97K) and PS (M_w = 160K) annealed for different times at 150 ℃. (a) PS (M_w = 97K) dead layer. (b) PS (M_w = 97K), 18 nm (red), 35 nm (violet), 300 nm (black); PS (M_w = 160K), 20 nm (pink) and 44 nm (green). (c) Thickness difference of dead layer and bulk PS. [20]

Napolitano et al. tried to explain the relationship between the annealing time and the T_g of PS as follows: The thickening process of the dead layer by increasing annealing time leads to a gradually filling of the empty sites at the polymer/substrate interface. This means more polymer chains tend to lie on the substrate. The conformations are shown in Fig. 1-6. The annealing process tunes the mobility of the polymer chains and leads to a larger polymer/substrate ratio. Larger polymer/substrate ratio means higher interfacial T_g.

Figure 1-6. The conformations of polymer chains at different annealing time. (a) PS (M_w = 97K) annealed for 7.5 mins. (b) PS (M_w = 97K) annealed for 2 h. (c) PS (M_w = 97K) annealed for 12 h. [20]

In another paper of Napolitano, the dependence of T_g as a function of the thickness of Poly(tert-butylstyrene) (PTBS) dead layers was studied [23]. The PTBS films were also spun-casted on aluminum substrates. A capacitive dilatometry was used to measure the temperature dependence of the capacitance of PTBS films with thickness of 78, 15, 7, and 5 nm. The thermal expansion coefficient in the direction normal to the film surface has an inverse proportionality between capacitance of the film so that the thickness of the PTBS dead layers can be obtained indirectly from the capacitance data. Fig. 1-7. shows their

capacitance data for PTBS dead layers, from which we can see the increase of the thickness of the film due to thermal expansion. The kinks in the data correspond to the T_g. The result shows that as the dead layer becomes thicker, T_g also increases.

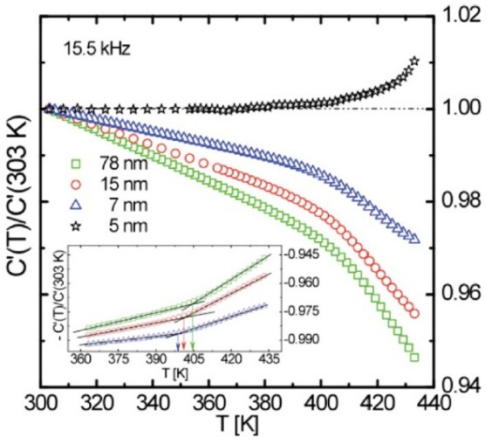

Figure 1-7. Thermal capacity evolution of PTBS dead layers with different thickness in different temperatures; the inset is the fitting of T_g. [23]

1.6 Research motivation and objectives

As discussed above, with a small amount of nanofiller added to a polymer matrix, the performance of polymer nanocomposite is superior relative to a pure polymer, and these advantages of nanocomposites have been put into industrial applications, including biomedical manufacture [24], fuel cell production [25] and many other areas. Also, recent researches on polymer thin films have shown that polymer thin films have various unique properties compared to bulks, which makes polymer thin film a promising topic for research. The understanding of the interaction between the polymer and the substrate is the key to explain the deviations of the polymer thin films from the bulks.

In this thesis, the effect of clay nanoparticle on PS dead layer will be studied to provide the understanding of the origin of the deviations. We aim to find the relationship between the annealing time and the thickness of PS-clay dead layers. Furthermore, by comparing the annealing time dependence of PS-clay dead layers with that of pure PS dead layers, we provide new insight into the mechanism how clay particles affect PS dead layers.

Chapter 2 Materials and Methods

2.1 Preparation of polymer solutions

The polymer solutions were prepared at room temperature. For the polystyrene solution, 0.2 g polystyrene (PS) (M_w = 290,000, M_w/M_n = 1.06, Pressure Chemical co.) was dissolved into 9.8 g toluene (99.5%, Sigma-Aldrich). For PS-clay solutions, we changed different mass ratios of PS : clay i.e., PS : clay = 100 : 1, 100 : 5 and 10 : 1. The organo clay 6A nanoparticles (Southern Clay Company, USA) were dissolved in toluene and then PS was added to the solutions. The solutions were left at room temperature for 24 h to make sure the solutions were well mixed.

2.2 Cleaning silicon wafers

We chose silicon as the substrate for polystyrene thin films, silicon wafers were cut into small pieces with size 2 cm × 2 cm. First of all, the silicon wafers were put into a beaker, then washed with distilled water for 5 times, making sure all silicon wafers were faced up. Next, we added 50 mL of distilled water, 50 mL of hydrogen peroxide (Fisher Chemical, H325-500) and 50 mL of ammonia hydroxide (Avantor Performance Materials) into the beaker. The third step was to heat up the beaker at 150 ℃. After 20 min, the solution was put into a waste bottle, leaving silicon wafers in the beaker. And we washed the wafers with distilled water again for 5 times. Next, hydrogen peroxide and sulfuric acid (Pharmco Aaper) were used to wash the wafers for 20 min at 150 ℃. The process of washing silicon wafers was done.

2.3 Preparation of PS and PS/clay thin films

We used a spin coater (Headway Research. lnc, Sarland, Texas) to prepare thin films. Before spin casting, silicon wafers was washed in diluted hydrofluoric acid (Sigma-Aldrich) for 15 sec to remove the SiO_2 layers and all polymer solutions were sonicated (Bransonic Co., Virginia) for 60 sec to achieve exfoliation of the clay platelets. After dropping several drops of polystyrene solutions on the entire silicon surface, the substrate was rotated at the speed of 2500 rpm for 20 sec. Spin-casting on substrates actually form non-equilibrium conformations of the polymer. Some diffusion experiments indicate that polymer chains in spin-casted films are less entangled [26]. However, annealing will help the polymer chains form an equilibrium and stable structure. So, after preparing the spin-cast samples, we put samples in a vacuum oven, set the temperature of 150 ℃, which was 50 deg above the bulk T_g of PS. After the long annealing process, we took out the samples and left them in air at the room temperature for fast quench.

2.4 Preparation of PS and PS/clay dead layers

We removed the PS by rinsing the thin films in toluene for 10 min at room temperature and repeated this rinsing process for several more times until the thickness of the dead layers finally reached equilibrium.

2.5 Measuring the thickness of the dead layers

An ellipsometer (Rudolph Research) was used to measure the thickness of the dead layers. Ellipsometry is a technique based on measurement of the change of the polarization of light after reflected or transmitted on the samples. During the measurement, a laser beam is used as the light source, and the light emitted by the laser will be polarized by a polarizer, then it hits the surface of the sample. After reflection, the reflected light passes a compensator and a second polarizer, and finally goes to a detector [27-29]. Fig. 2-1 is a schematic diagram of the principle of ellipsometry. In this experiment, the index of refraction 1.575 was used for pure polystyrene. For PS-clay dead layers, we assume that the index of refraction is the same with PS because the amount of clay are at most 10%. We can see that the dead layers of PS thin films are almost flat and homogeneous, while the dead layers of PS-clay thin films have clay particles on the surface.

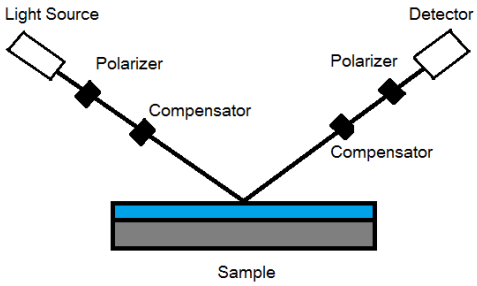

Figure 2-1.Schematic diagram of ellipsometry

2.6 Obtaining surface information of dead layers

The technique used to get morphological information of the dead layers is atomic force microscopy (AFM) (Digital Instruments, USA), which is a type of high resolution scanning probe microscopy, consisting of a cantilever with a sharp tip. When the tip gets close to the surface of a sample, the force between the tip and the sample changes and leads to a deflection of the cantilever. The deflection is measured by a laser beam reflected from the top surface of the cantilever. This technique provides us the topography of the dead layer, such as clay dispersion, thickness difference, morphology and friction information. Images were analyzed by Nanoscope programming.

2.7 Using supercritical carbon dioxide to change the structure of PS-clay dead layers

Supercritical carbon dioxide ($scCO_2$) is an environmentally benign solvent, nonflammable and nontoxic. The supercritical condition is achieved at temperatures and pressures above their critical points. Under supercritical conditions, CO_2 has the behavior of both gas and liquid, with very high diffusivity like gas and liquid-like density. The critical temperature for CO_2 is 31.3 ℃ and critical pressure is 7.38 MPa. The process of $scCO_2$ is shown in Fig. 2-2 [30]. We aimed to seek how $scCO_2$ would affect the structures

of the dead layers.

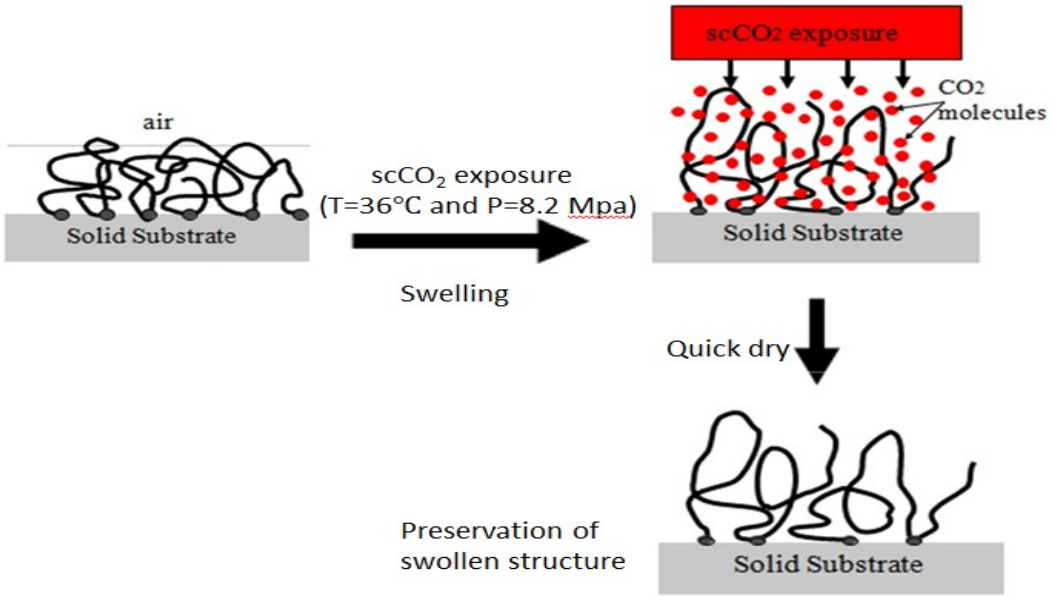

Figure 2-2. Diagram of the $scCO_2$ process [30]

2.8 X-ray reflectivity to determine the thickness of PS-clay dead layers

To get structural information from the dead layers of PS-clay thin film, X-ray reflectivity experiments were carried out at the beam line X10B in Brookhaven National Lab. X-ray reflectivity is a surface analytical technique widely used in chemistry, materials science and physics to characterize surface/interface structures [31-32]. The principle of the X-ray reflectivity is an incident X-ray beam hits the surface of the sample, the X-ray reflects and the information of the reflected beam will be collected by a detector. During the measurement, the tilt of the sample holder leads to the change in the incident angle of X-ray beam, and the reflected beam from the film is monitored by the detector. Fig. 2-3 is a schematic diagram of X-ray reflectivity.

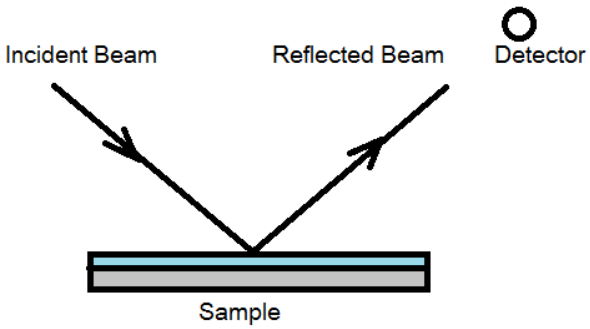

Figure 2-3. Schematic diagram of X-ray reflectivity

Chapter 3 Results and Discussion

3.1 Annealing time dependence of the thickness of PS and PS-clay dead layers

For pure PS dead layers, 8 dead layers were prepared and tested with different annealing times of 2, 5, 8, 10, 14, 22, 24 and 48 h. The thickness of the dead layers is plotted in Fig. 3-1.

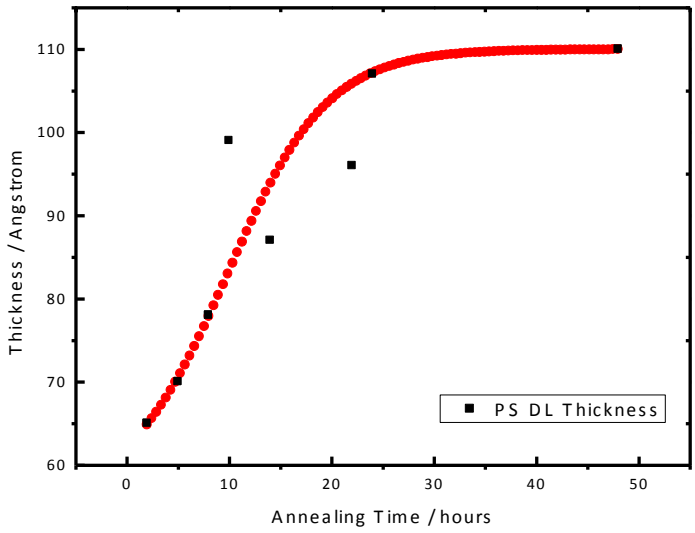

Figure 3-1. Annealing time dependence of the thickness of PS dead layer

The measurement of the thickness of a PS dead layer by ellipsometry is quite straight forward because the surface of the dead layer is almost homogeneous, even when we choose different sites on the dead layer, the thickness difference is still within 2 Å. This behavior is similar to the result reported by Fujii et al. [18], as the increase of annealing time, the thickness of PS dead layers increases, and becomes constant after 24 h. We believe 24 h is enough for PS dead layer to reach its equilibrium thickness, which is approximately 11 nm. This thickness is thicker than the equilibrium dead layer reported by Fujii et al. because our M_w is different from theirs. This result is consistent with Fujii's result of the dependence of R_g on the thickness of PS dead layer, because higher molecular weight means larger R_g.

We used the same protocol to prepare PS-clay dead layers as for the pure PS. However, the introducing of clay particles makes the ellipsometry measurements difficult. Although the sonication process for PS-clay solutions was carried out to exfoliate clay nanoparticles [6], we found that the aggregations of clay particles still exist in the dead layers, resulting in rough surface of PS-clay dead layers. Fig. 3-2 shows the annealing time dependence of the average thickness of PS-clay dead layer.

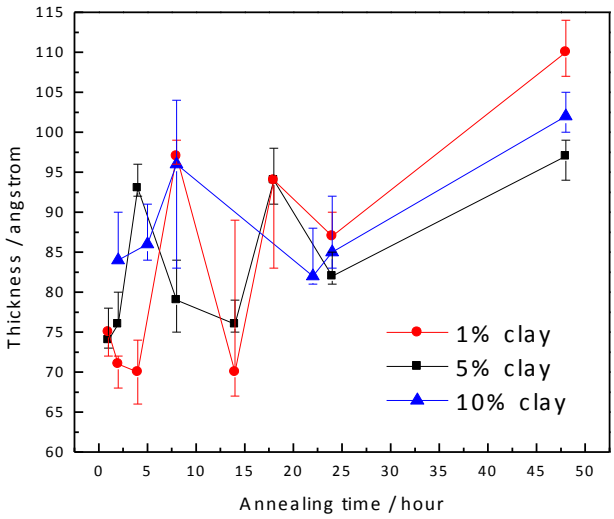

Figure 3-2. Annealing time dependence of the average thickness of PS-clay dead layer

In contrast to the pure PS dead layers, the thickness of the PS-clay dead layers fluctuates as the annealing time increases. Nevertheless, we can still observe the growth of the PS-clay dead layers. There are still obvious thickness differences between samples annealed for less than 5 h and samples annealed for 48 h, which implies the behavior of polymer chains in PS-clay dead layers is similar to that in pure PS dead layers. If we compare the thickness of PS-clay dead layers annealed for 24 h with that for 48 h, the average thickness annealed for 48 h is larger than that annealed for 24 h, indicating the 24 h annealing time is not enough for PS-clay dead layers to reach its equilibrium. This is different from the behavior of the pure PS because we have the same thickness of PS dead layers with annealing time 24 h and 48 h. Embedding the clay nanoparticles, the PS-clay dead layers take more time to form its equilibrium. Namely, the clay particles decrease the mobility of PS chains. During the annealing process, some PS chains diffuse into the interlayers of the clay particles and form network-like structures [1, 10-12], preventing the polymer chains from moving away.

3.2 X-ray reflectivity for PS-clay dead layers

As mentioned before, the surface of the PS-clay dead layers are quite rough, and the thickness measured by ellipsometry may contain large errors. In this study, we also used X-ray reflectivity to characterize the thickness of the dead layers. Representative X-ray reflectivity profiles and fourier transform profiles are shown in Fig. 3-3.

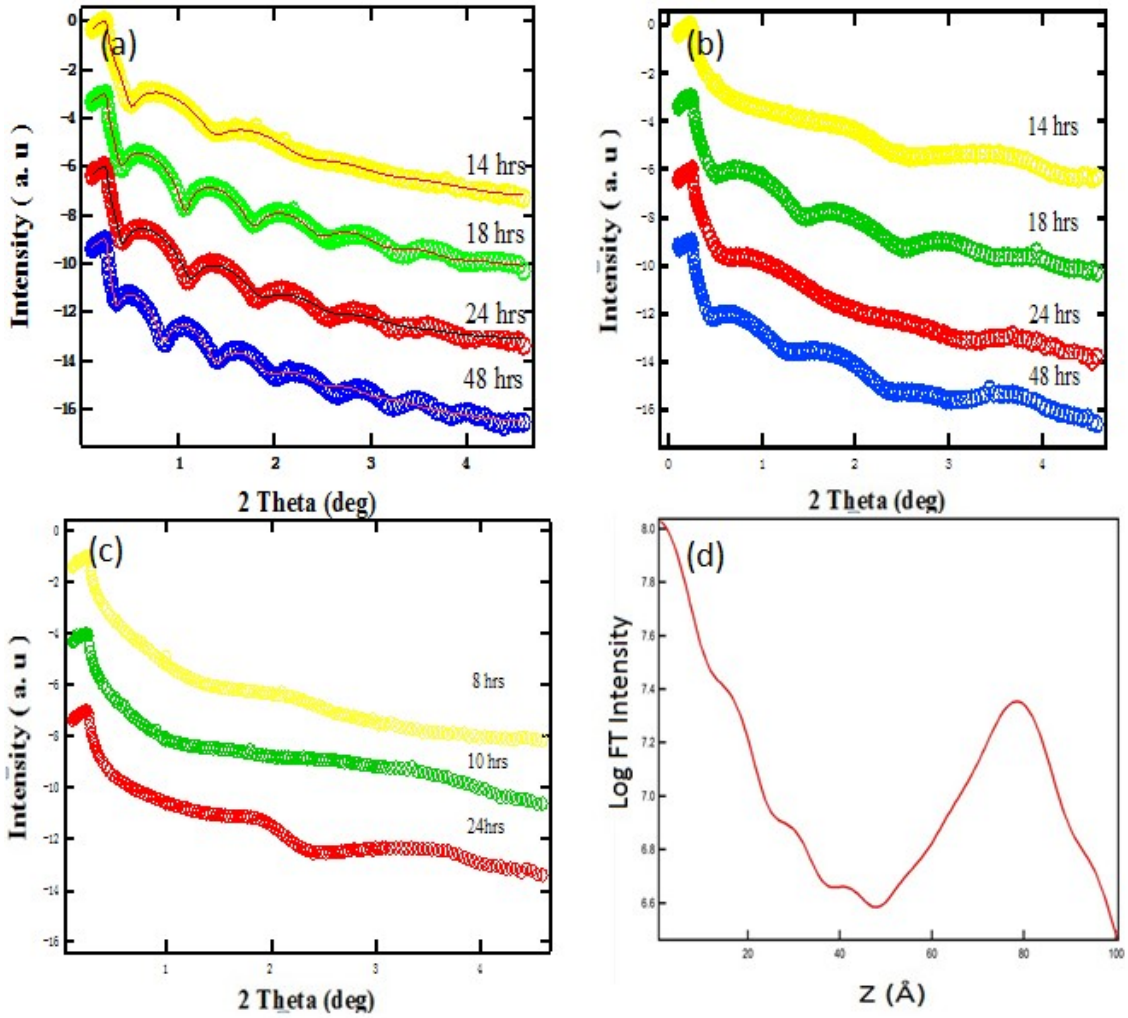

Figure 3-3. (a) X-ray reflectivity data for samples with 1% clay, there are nice fringes for this group of samples, the solid lines are the fitting curves. (b) X-ray reflectivity data for samples with 5% clay, only some of the samples have good fringes. (c) X-ray reflectivity data for samples with 10% clay, there are almost no fringe for this group of samples. (d) The fourier transform profile of a sample with 1% clay.

As we can see for all PS/clay (1% wt.) dead layers have nice fringes, implying the smooth surface. However, as we added more clay to polymers, the X-ray profiles do not exhibit the fringes. This indicates the strong aggregation of clay with high concentration of clays.

There are multiple peaks in the fuorier transform profile of the dead layer (Fig. 3-3 (d)), indicating multiple interlayers in the dead layer, which makes the fitting process complex. To simplify the fitting, we assume there are four layers in the samples (silicon substrate, oxide layer, PS and clay), the thickness dependence of the dead layers on the annealing time is plotted in Fig. 3-4.

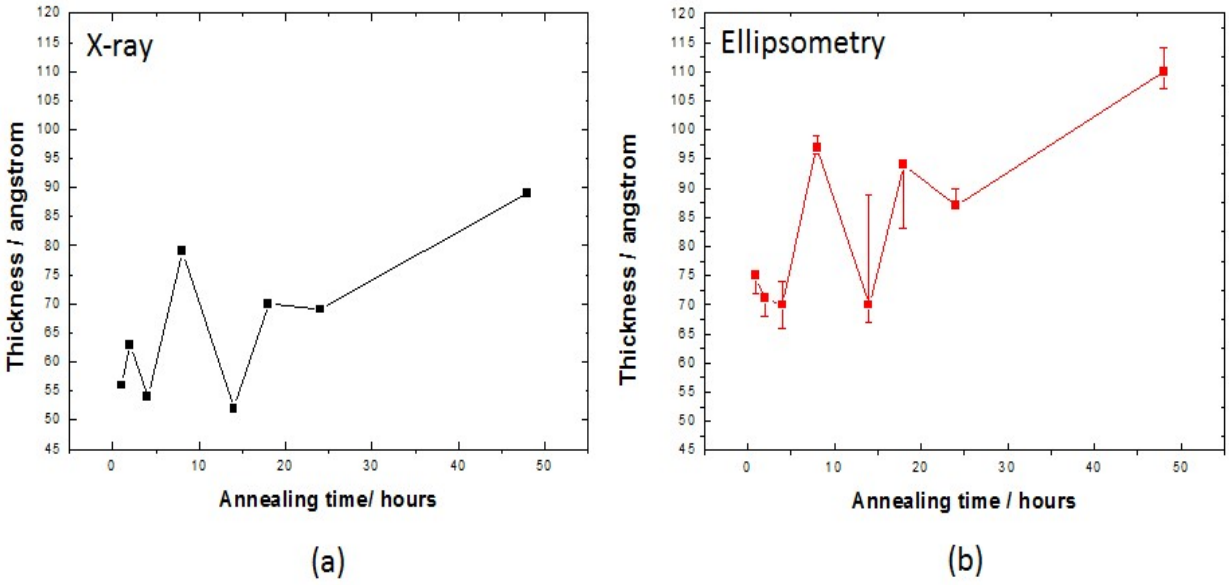

Figure 3-4. Annealing time dependence of the thickness of dead layers with 1% clay. (a) The fitting data from X-ray reflectivity; (b) Data measured by Ellipsometry.

Comparing the experimental data from the respective technique, we can see the similar trend and the difference in the thickness between them is around 2 nm. Also from the X-ray data, we can confirm that 24 h annealing time is not sufficient for the PS-clay dead layers to reach equilibrium.

We also tried to characterize the temperature dependence of the thickness of the PS-clay dead layers. The result is shown in Fig. 3-5.

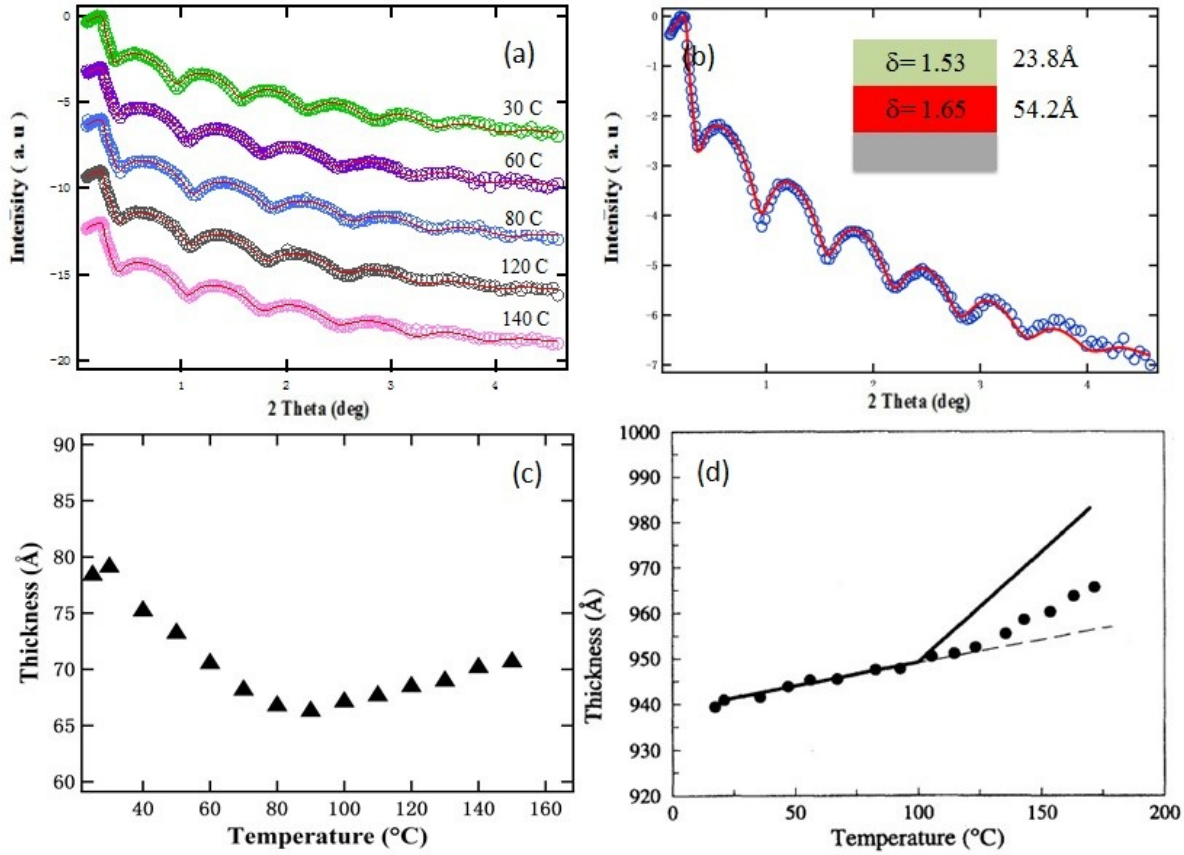

Figure 3-5. High temperature experiment for the sample with 1% clay, with annealing time of 24 h. (a) Representative X-ray data (circles) and fitting data (solid line) for the sample at different temperatures. (b) The x-ray data (circles) and fitting data (solid line) for the sample at room temperature and the thickness for the two layers of polymer and clay. (c) Temperature dependence of the thickness of the dead layer. (d) Typical PS thin film high temperature X-ray data. [17]

As we increase the temperature, the total thickness of the dead layer decreased up to 80 ℃, and then increased again up to 150 ℃. A typical pure PS thin film usually has an increase of the thickness with the increase of the temperature, and when the temperature is above the T_g, the increase of the thickness becomes faster and we can observe a kink on the profile. (Fig. 3-5 (d))

3.3 Surface information of PS-clay dead layer

The images obtained by AFM tell the difference between a pure PS dead layer and a PS-clay dead layer. The height image of a typical PS dead layer shows the surface is almost homogeneous, Fig. 3-6 (a). In contrast, a PS-clay dead layer has clay particles at the surface, which makes the surface rough.

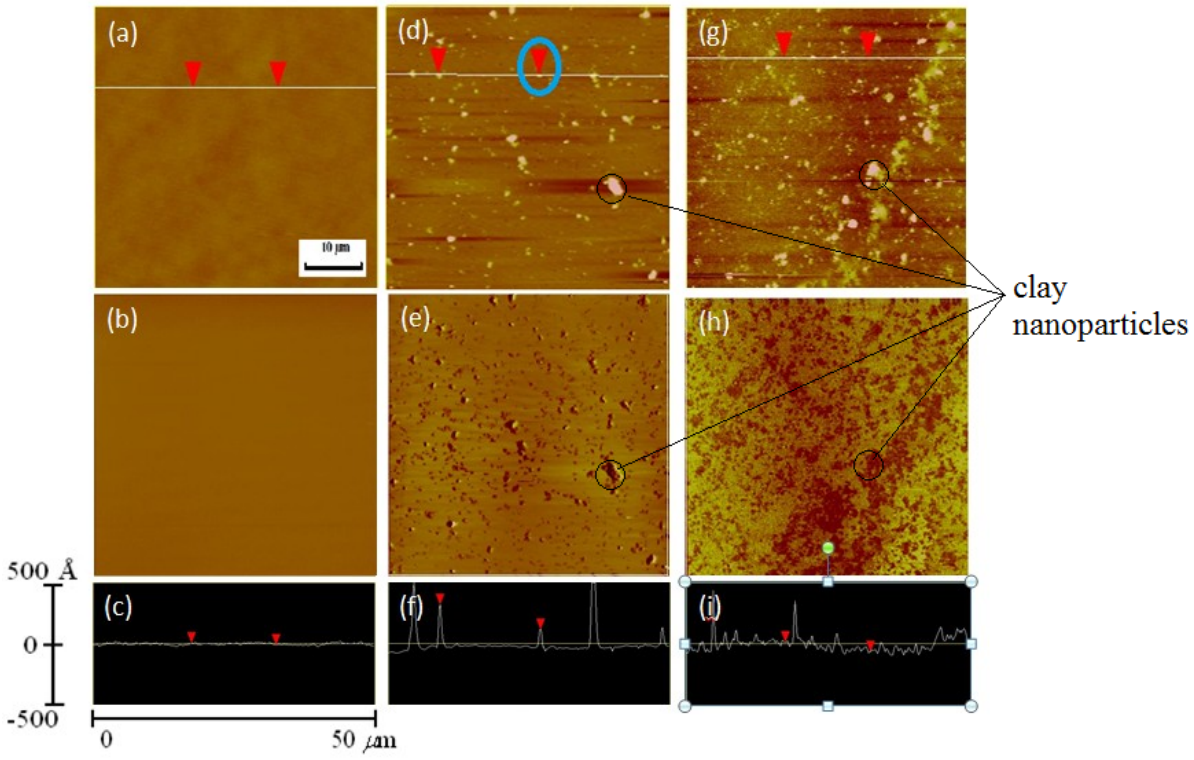

Figure 3-6. AFM images of PS and PS-clay dead layers. (a) Height image of PS dead layer. (b) friction image of PS dead layer. (c) Cross-section information of PS dead layer. (d) Height image of PS-clay dead layer with 1% clay. (e) Friction of PS-clay dead layer with 1% clay. (f) Cross-section information of PS-clay dead layer with 1% clay. (g) Height image of PS-clay dead layer with 10% clay. (h) Friction of PS-clay dead layer with 10% clay. (i) Cross-section information of PS-clay dead layer with 10% clay. The small clay particle on (b), which is marked by a blue circle, has a height of 14nm and width of 100nm. If we consider the height for a single clay is 3nm, there is about 4 – 5 clay particles aggregating on that spot.

As shown in Fig. 3-6 (d), (g), the bright area in the height images corresponds to the clay nanoparticles. And in Fig. 3-6 (f), (i), the cross-sections along the lines indicate there are more aggregations in the dead layer with higher clay concentrations.

Now the question is whether the clay particles attach to the silicon substrate or the polymer? We proposed three possible situations to express the internal structures of the PS-clay dead layers. (Fig. 3-7)

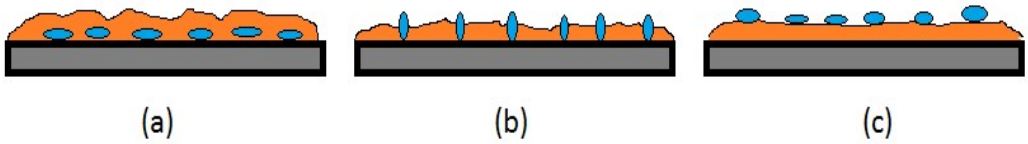

Figure 3-7. Three possible models for the internal structure of PS-clay dead layers. The blue ellipses stand for the clay nanoparticles, the orange parts stand for PS, and the gray rectangles stand for silicon substrates. (a) Model A, clay particles are covered by polymer on the substrate. (b) Model B, clay particles stand on silicon substrate, with PS surrounded. (c) Model C, PS covers the surface of silicon substrate with clay particles on the top of PS.

We can rule out the model A because if the top surface of the dead layer is covered by PS, the surface friction of a PS-clay dead layer should be the same in the friction image. However, Fig. 3-6 (e), (h) indicate that the friction of PS and clay are different. We cannot tell which model is appropriate for the PS-clay dead layers. However, based on the above experimental results, $scCO_2$ experiments were conducted to answer the question.

3.4 Swelling behavior of PS-clay dead layer

The idea to use $scCO_2$ for the PS-clay dead layer is based on the fact that $scCO_2$ can be used as a screening solvent between PS and Si substrate. We placed a PS-clay dead layer in the high pressure chamber at the condition of 8.2 Mpa and 36 ℃ for 2 h, where the plasticization effects and screening effects become profound [33].

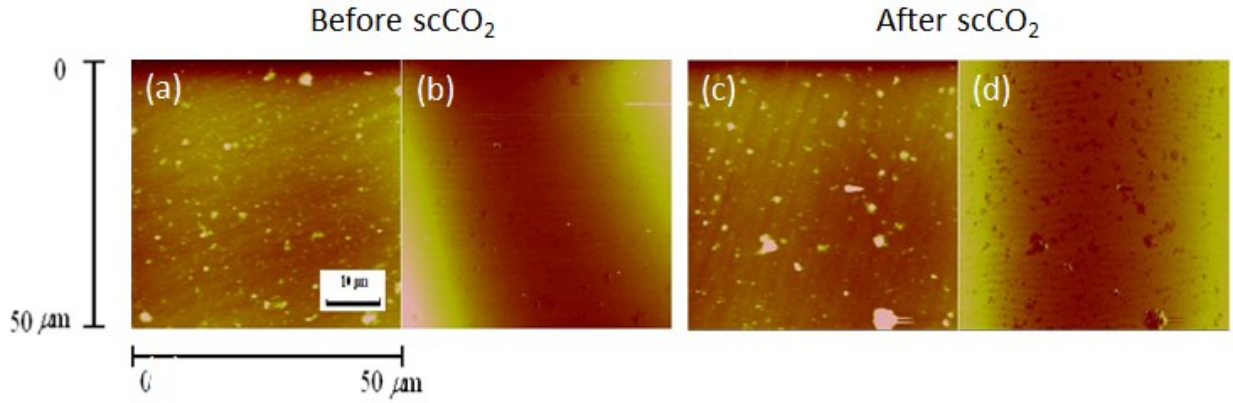

Figure 3-8. AFM images of PS-clay dead layers with 1% clay before and after the $scCO_2$ process. (a) Height image of PS-clay dead layer before the $scCO_2$ process. (b) Friction image of PS-clay before the $scCO_2$ process. (c) Height image of PS-clay dead layer after the $scCO_2$ process. (d) Friction image of PS-clay after the $scCO_2$ process.

By comparing the friction images of PS-clay dead layers before the $scCO_2$ process (Fig. 3-8 (b)) and after the $scCO_2$ process (Fig. 3-8 (d)), we can see the surface friction of the PS-clay dead layer becomes different. Therefore our assumption is after the $scCO_2$ treatment the polymer became softer such that the clay particles became relatively harder. This assumption is further verified by measuring the thickness of the dead layers. The thickness of the sample, which was 60 Å before the $scCO_2$ process, and increased to 82 Å after the $scCO_2$ process. This means $scCO_2$ makes the dead layer swollen. The dead layer after the $scCO_2$ process was rinsed by toluene one more time, we found that the thickness decreased to 51 Å, and we could still observe clay particles at the surface. This proposes that the model B is more reasonable. But the decrease of the thickness is only 9 Å. This may result from the error of the ellipsometry, and further experiments are needed to prove this hypothesis. We increased the times of cycles of $scCO_2$ process and toluene rinsing process for the dead layer. A PS-clay dead layer with initial thickness of 87 Å was prepared, after 5 times of the $scCO_2$ process and toluene rinsing process, the thickness of the dead layer decreased to 65 Å. And we observed clay particles on the dead layer. This indicates even the top surface layer was rinsed by toluene, clay particles choose to stay on the dead layer. This further proposes the model B is more reasonable.

Chapter 4 Conclusions and Future Work

We have investigated the effect of organo clay nanoparticles on the structures/properties of PS dead layers. In order to characterize such thin layers, X-ray， AFM, ellipsometry were used. By analyzing the data of the annealing the time dependence of the thickness of the PS-clay dead layers, we have the following conclusions: 1) The thickness of the dead layers increases with the increase of the annealing time; 2) The equilibrium time for the PS/clay dead layers is much longer than that of pure PS dead layers. This can be explained by the fact that the clay nanoparticles suppress the chain mobility of PS.

X-ray reflectivity results showed that samples with 1% clay nanoparticles exhibit nice fringes on the reflectivity data, indicating the formation of a smooth surface, while clay particles with weight fraction more than 5% cause significant rough surface. The high temperature X-ray experiments for the PS/clay dead layers showed a decrease in the thickness up to 80 ℃ then increase up to 150 ℃. We did not see any indication of T_g of the polymer.

By using $scCO_2$, we aimed to understand the interaction of the PS/clay and silicon substrate. The results indicated there is a good affinity between clay and silicon substrate. We proposed three possible models for the internal structure of PS-clay dead layers. And by rinsing the dead layers after the $scCO_2$ process, we observed decrease of the thickness of the dead layers, and clay particles were still on the surfaces of the dead layers. This proposes that the model B is more reasonable for the PS-clay dead layers.

In the future experiments, different clay nanoparticles with different affinity with Si substrate should be used to see how different clay nanoparticles can alter the structures/properties of PS dead layers. In addition, aggregations still exist in the PS-clay dead layers, better methods are needed to help the exfoliation of the clay nanoparticles.

Bibliography

[1] T. Kashiwagi, R. H. Harris Jr, X. Zhang, R. M. Briber, B. H. Cipriano,S. R. Raghavan, W. H. Awad, J. R. Shields, Flame retardant mechanism of polyamide 6–clay nanocomposites, Polymer, 45, 881-891, 2004.

[2] J. Ahn, W. Chung, I. Pinnau, M. D. Guiver, Polysulfone/silica nanoparticle mixed-matrix membranes for gas separation, Journal of Membrane science,314 123–133, 2008.

[3] B. K. Kim, J. W. Seo, H. M. Jeong, Morphology and properties of waterborne polyurethane/clay Nanocomposites, European Polymer Journal, 39, 85–91, 2003.

[4] J. Li, S. A. schwarz, Y. Ji, M. H. Rafailovich, J. Sokolov, Effect of clay platelet orientation on spin cast nanocomposite films, Appl. Phys. Lett. 89, 111917 , 2006 .

[5] A. Olad, Advances in Diverse Industrial Applications of Nanocomposites, ISBN: 978-953-307-202-9.

[6] P. C. LeBaron, Z. Wang. & T. J. Pinnavaia, Polymer-layered silicate nanocomposites: an overview, Appl. clay sci., 15, 11-29, 1999.

[7] S. A. Solin, Clays and clay intercalation compounds: Properties and Physical Phenomena, Annu. Rev. Mater. sci. , 27, 89–115, 1997.

[8] E. P. Giannelis, R. Krishnamoorti, E. Manias, Polymer-Silicate Nanocomposites: Model Systems for Confined Polymers and Polymer Brushes, Adv. Polym. sci. 118, 108 , 1999.

[9] J. Zhang, C. A. Wilkie, Preparation and flammability properties of polyethylene–clay Nanocomposites, Polymer Degradation and Stability 80, 163–169, 2003.

[10] M. Zanetti, S. Lomakin, G. Camino, Polymer layered silicate nanocomposites, Macromol. Mater. Eng. 279, 1–940, 2000.

[11] Q. T. Nguyen, D. G. Baird, Preparation of Polymer–Clay Nanocomposites and Their Properties, Adv Polym Techn. 25, 270–285, 2006.

[12] Professor J.N. Hay and S.J. Shaw, A Review of Nanocomposites, 2000.

[13] J. L. keddie, R. A. L. jones, and R. A. cor, Size-Dependent Depression of the Glass Transition Temperature in Polymer Films, Europhys. Lett., 27, 59-64, 1994.

[14] G. Reiter, Dewetting as a Probe of Polymer Mobility in Thin Films, Macromolecules, 27, 3046-3052, 1994.

[15] O. K. C. Tsui, Y. J. Wang, F. K. Lee, C. H. Lam, and Z. Yang, Equilibrium Pathway of Spin-Coated Polymer Films, Macromolecules, 41, 1465-1468, 2008.

[16] M. K. Sanyal, J. K. Basu, A. Datta and S. Banerjee, Determination of small fluctuations in electron density profiles of thin films: Layer formation in a polystyrene film, Europhys. Lett., 36, 265-270, 1996.

[17] W. E. Wallace, J. H. van Zanten, and W. L. Wu, Influence of an impenetrable interface on a polymer glass-transition temperature, Phys. Rev.E, 52, 3329–3332, 1995.

[18] Y. Fujii, Z. Yang, J. Leach, H. Atarashi, K. Tanaka, and O. K. C. Tsui, Affinity of Polystyrene Films to Hydrogen-Passivated Silicon and Its Relevance to the Tg of the Films, Macromolecules, 42, 7418–7422, 2009.

[19] C. J. Durning, B. O'Shaughnessy, and U. Sawhney, Adsorption of Poly(methyl methacrylate) Melts on Quartz, Macromolecules, 32, 6772-6781, 1999.

[20] S. Napolitano, M. Wübbenhorst, The lifetime of the deviations from bulk behaviour in polymers confined at the nanoscale, Nature Communications, 2, 260, 2011.

[21] T. Koga, N. Jiang, P. Gin, M. K. Endoh, S. Narayanan, L. B. Lurio, and S. K. Sinha, Impact of an Irreversibly Adsorbed Layer on Local Viscosity of Nanoconfined Polymer Melts, PRL 107, 225901, 2011.

[22] S. Napolitano and M. Wu1bbenhorst, Dielectric Signature of a Dead Layer in Ultrathin Films of a Nonpolar Polymer, J. Phys. Chem. B, 111, 9197-9199, 2007.

[23] S. Napolitano, A. Pilleri, P. Rolla, and M. Wu, Unusual Deviations from Bulk Behavior in Ultrathin Films of Poly(tert-butylstyrene): Can Dead Layers Induce a Reduction of Tg? , ACS Nano, 4 (2), 841–848, 2010.

[24] A. R.. Hule and D. J. Pochan, Polymer Nanocomposites for Biomedical Applications, MRS BULLETIN, 32, 354-358, 2007.

[25] G. G. Kumar and K. S. Nahm, Polymer Nanocomposites - Advances in Nanocomposites - Synthesis, Characterization and Industrial Applications, ISBN: 978-953-307-165-7.

[26] B. B. Sauer and D. J. Walsh, Effect of Solvent Casting on Reduced Entanglement Density in Thin Films Studied by Ellipsometry and Neutron Reflection, Macromolecules, 27, 432-440, 1994.

[27] AFPO Group, Laboratory of Solid State Physics, ELLIPSOMETRY, CNRS & Universite Paris.

[28] R. M. A. Azzam and N. M. Bashara, Ellipsometry and Polarized Light, Elsevier science Pub Co., ISBN 0-444-87016-4, 1987.

[29] A. Roeseler, Infrared Spectroscopic Ellipsometry, Akademie-Verlag, Berlin, ISBN 3-05-500623-2, 1990.

[30] T. Koga, J. Jerome, M. H. Rafailovich, B. Chu, J. Douglas, S. Satija, Supercritical fluid processing of polymer thin films: an X-ray study of molecular-level porosity, Advances in colloid and interface science, 01, 128-130:217-26, 2006.

[31] J. A. Nielsen, Elements of Modern X-Ray Physics, Wiley, New York, 2001.

[32] J. Daillant, A. Gibaud, X-Ray and Neutron Reflectivity: Principles and Applications. Springer, 1999.

[33] M. Asada, P.r Gin, M. K. Endoh, S. K. Satija and T. Koga, Surface Segregation of Nanoparticles Driven by Supercritical Carbon Dioxide, Journal of Physics: Conference Series 272 , 12-13, 2011.